



Efficient impulse noise detection method with ANFIS for accurate image restoration

Ilke Turkmen *

Erciyes University, Civil Aviation School, Department of Aircraft Electrical and Electronics, 38039 Kayseri, Turkey

ARTICLE INFO

Article history:

Received 28 July 2007

Accepted 2 February 2010

Keywords:

Impulsive noise

Impulse noise detector

ANFIS

ABSTRACT

This paper proposes a novel adaptive neuro-fuzzy inference system (ANFIS) based impulse detection method for the restoration of images corrupted by impulse noise (IN). After the corrupted pixels detected by proposed detector, the Median filtering is performed for only these pixels. The performance of the proposed neuro-fuzzy detector based median filter (NFD MF) is evaluated on different test images and compared with 14 different comparison filters from the literature. Experimental results show that the proposed filter shows better performance than the comparison filters in the cases of being effective in noise suppression and detail preservation, especially when the noise ratio is very high.

© 2010 Elsevier GmbH. All rights reserved.

1. Introduction

Images are often corrupted by impulse noise (IN) due to errors generated in noisy sensors or communication channels. IN could degrade the image quality and cause great loss of image details. So it is important effectively to reduce noise from the image to facilitate subsequent image processing operations, such as edge detection, image segmentation, and object recognition. The goal of noise removal is to suppress the noise while preserving image details. To this end, a large number of algorithms [1–28] have been proposed to remove IN.

The median filter is one of the most popular nonlinear filters for removing IN because of its good denoising power [1] and computational efficiency [2]. Median filter utilize the rank order information of the pixels contained in the filtering window. It attempts to remove impulse noise by changing the luminance value of the each pixel in the image by the median value in its neighborhood. However, when the noise level is over 50%, some details and edges of the original image are smeared by the filter [3]. In order to overcome this drawback, different remedies of the median filter have been proposed. In [4] center weighted median filter (CWM) giving more weight only to the center value in the filtering window was presented. A nonlinear filter called tri-state median filter (TSM) combining the standard median filter with the CWM filter was proposed in [5] for suppressing impulse noise. The nonlinear LUM (low–upper–middle) smoothers, which are a subclass of LUM filters [6–8] that take advantage of the computational efficiency of order-statistics based operators, have

been shown to be equivalent to the CWM. Methods mentioned above can achieve good results at low noise density, but their denoising performances are unsatisfactory at high noise density. These methods are implemented uniformly across the image and thus tend to modify both noisy and noise-free pixels. Consequently, the effective removal of IN is often accomplished at the expense of blurred and distorted features, thus removing fine details in the image.

To avoid the damage of good pixels, the switching strategy is introduced by some recently published papers [9–14]. The switching scheme consists of the following two parts: the first part is an impulse detector which determines whether a target pixel is contaminated and the second part is a noise reduction filter which modifies only the pixels determined to be IN by the first part. In order to achieve accurate image restoration with the switching scheme, an accurate impulse detector is required, because the impulse detection result is utilized for the noise reduction filter.

Over the last few years, artificial intelligence-based nonlinear techniques such as neural networks and fuzzy systems have been attractive alternatives to classical noise detection and reduction techniques [15–28]. In [16] iterative fuzzy control-based filtering (IFCF) method was presented. The IFCF filter was designed for the removal of both impulse noise and Gaussian noise. This filtering approach is mainly based on the idea of not letting each point in the area of concern being uniformly fired by each of the basic fuzzy rules. The extended iterative fuzzy control-based filter (EIFCF) and the modified iterative fuzzy control-based filter (MIFCF) were also presented in [16]. EIFCF, which is a slightly modified version of the IFCF, was designed to counter the blurring of the image. In IFCF, the image gets more blurred after each iteration. MIFCF was designed to avoid this drawback. Smoothing

* Tel.: +90 352 437 57 44; fax: +90 352 437 57 84.
E-mail address: titi@erciyes.edu.tr

fuzzy control based filter (SFCF) presented in [17] is a noniterative version of IFCF. The advantage of a noniterative filter is that the corresponding algorithm has to be applied only once and there is no need for a stopping criterion. In [18], fuzzy inference rule by else-action filter (FIRE) was designed to remove impulse noise. The FIRE filter uses fuzzy rules to estimate degree of noisy pixels and calculates a correction term based on this estimation. Piecewise linear FIRE (PWL-FIRE) filter, based on piecewise linear fuzzy sets whose shapes are dynamically adapted depending upon the local characteristics of the image was presented in [19]. In [22], adaptive weighted fuzzy mean (AWFM) filter which is capable of removing high density Gaussian impulse noise in polluted images was presented. Asymmetrical triangular fuzzy filter with moving average center (ATMAV) was presented in [24]. In a given neighborhood, the ATMAV filter takes into account the deviation of the pixel value with the mean value and replaces the noisy pixel with a fitting output based on triangular membership function.

The fuzzy system based methods given above well suited to model the uncertainty that occurs when both noise removal and detail preservation are required. However, when the images are highly corrupted, discovering the rule-base structure becomes quite difficult. In order to overcome this difficulty, many methods [23,25–28] based on adaptive neuro-fuzzy inference system (ANFIS) are proposed, which make full use of the ability of neural networks to learn from examples. With suitable and sufficient training, they can preserve the image details during noise detection and removal.

The problem in the literature is that a method that is as simple as possible for detecting IN should be obtained, but the filtering results obtained by using these detected pixels must be very good. In this paper, a new IN detector using ANFIS method [29,30] is proposed. First, the parameters related to the IN detection are determined, and then the noisy pixels depending on these parameters are determined by using the ANFIS. After the application of the detector, IN removal operator focuses only on those pixels, i.e. the filtering concentrated on the real IN pixels. Advantages of the proposed method are its simplicity and accuracy. The rest of the paper is organized as follows: the detail of the ANFIS is given in Section 2. The proposed impulse detector is defined in Section 3 and finally, simulation results and conclusions are presented in Sections 4 and 5, respectively.

2. Adaptive neuro-fuzzy inference system (ANFIS)

The ANFIS [29,30] is a multilayer feed-forward network, which uses neural network learning algorithms and fuzzy reasoning to map an input space to an output space. While fuzzy logic performs an inference mechanism under cognitive uncertainty, computational neural networks offer advantages, such as learning, adaptation, fault tolerance, parallelism and generalization. To enable a system to deal with cognitive uncertainties in a manner more like humans, neural networks have been engaged with fuzzy logic, creating a new terminology called “neuro-fuzzy method”. ANFISs are fuzzy models put in the framework of adaptive systems to facilitate learning and adaptation. Such systems can be trained without need for the expert knowledge usually required to design the standard fuzzy logic.

A typical architecture of ANFIS is depicted in Fig. 1, in which a circle indicates a fixed node, whereas a square indicates an adaptive node. For simplicity, it was assumed that the FIS has two inputs x and y and one output z . The ANFIS used in this paper implements a first-order Sugeno fuzzy model. For this model, a

typical rule set with two fuzzy if–then rules can be expressed as

$$\text{Rule 1 : If } x \text{ is } A_1 \text{ and } y \text{ is } B_1 \text{ then } z_1 = p_1x + q_1y + r_1 \quad (1)$$

$$\text{Rule 2 : If } x \text{ is } A_2 \text{ and } y \text{ is } B_2 \text{ then } z_2 = p_2x + q_2y + r_2 \quad (2)$$

where A_i and B_i are the fuzzy sets in the antecedent, and p_i , q_i , and r_i are the design parameters that are determined during the training process. As in Fig. 1, the ANFIS consists of five layers with the output of the nodes in each respective layer is represented by O_i^j where i is i th node of layer l .

Layer 1: Every node i in the first layer employs a node function given by

$$O_i^1 = \mu_{A_i}(x), \quad i = 1,2 \quad (3a)$$

$$O_i^1 = \mu_{B_{i-2}}(y), \quad i = 3,4 \quad (3b)$$

where $\mu_{A_i}(x)$ and $\mu_{B_{i-2}}(y)$ can adopt any fuzzy membership function (MF). The current study utilized the triangular MF given as follows:

$$\text{triangle}(x; a, b, c) = \begin{cases} 0, & x \leq a \\ \frac{x-a}{b-a}, & a \leq x \leq b \\ \frac{c-x}{c-b}, & b \leq x \leq c \\ 0, & c \leq x \end{cases} \quad (4)$$

where $\{a_i, b_i, c_i\}$ is the parameter set that changes the shapes of the MF. Parameters in this layer are referred to as *the premise parameters*.

Layer 2: Each node in this layer calculates the firing strength of a rule via multiplication:

$$O_i^2 = \omega_i = \mu_{A_i}(x)\mu_{B_i}(y), \quad i = 1,2 \quad (5)$$

Layer 3: The i th node in this layer calculates the ratio of the i th rule’s firing strength to the sum of all rules’ firing strengths:

$$O_i^3 = \bar{\omega}_i = \frac{\omega_i}{\omega_1 + \omega_2}, \quad i = 1,2 \quad (6)$$

where $\bar{\omega}_i$ is referred to as *the normalized firing strengths*.

Layer 4: In this layer, each node has the following function:

$$O_i^4 = \bar{\omega}_i z_i = \bar{\omega}_i(p_i x + q_i y + r_i), \quad i = 1,2 \quad (7)$$

where $\bar{\omega}_i$ is the output of layer 3, and $\{p_i, q_i, r_i\}$ is the parameter set. Parameters in this layer are referred to as *the consequent parameters*.

Layer 5: The single node in this layer computes the overall output as the summation of all incoming signals, which is expressed as

$$O_1^5 = \sum_{i=1}^2 \bar{\omega}_i z_i = \frac{\omega_1 z_1 + \omega_2 z_2}{\omega_1 + \omega_2} \quad (8)$$

Thus an adaptive network has been constructed. The proposed ANFIS IN detector is based upon Jang’s ANFIS [29], which is a fuzzy inference system implemented on the architecture of a five-layer feed forward network. In the paper, the hybrid learning algorithm, which combines the least square method (LSM) and the back-propagation (BP) algorithm, is used to rapidly train and adapt the FIS. The algorithm converges faster since it reduces the dimension of the search space of the BP algorithm. From the architecture of ANFIS, it is observed that if the values of the premise parameters are fixed, the overall output can be expressed as a linear combination of the consequent parameters:

$$z = (\bar{\omega}_1 x)p_1 + (\bar{\omega}_1 y)q_1 + (\bar{\omega}_1)r_1 + (\bar{\omega}_2 x)p_2 + (\bar{\omega}_2 y)q_2 + (\bar{\omega}_2)r_2 \quad (9)$$

The LSM can be used to obtain the optimal values of the consequent parameters. When the premise parameters are not fixed, the search space becomes larger and the convergence of training becomes slower. The hybrid learning algorithm is adopted to solve this problem. The algorithm has a two-step

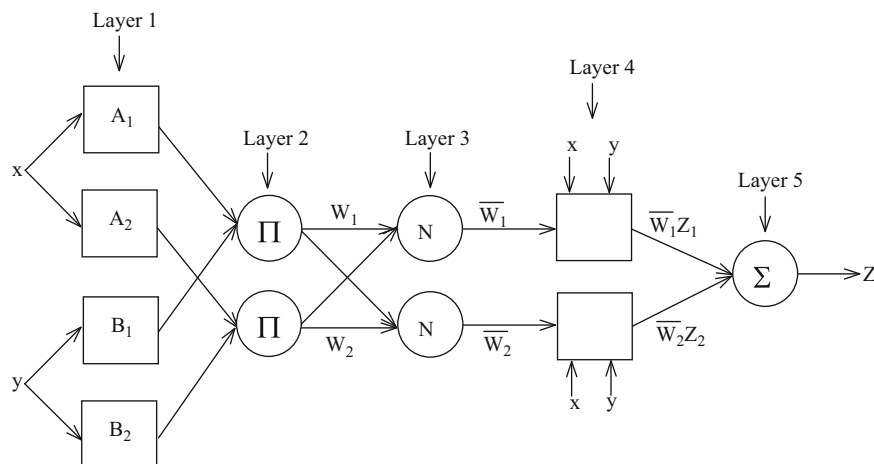


Fig. 1. Architecture of ANFIS.

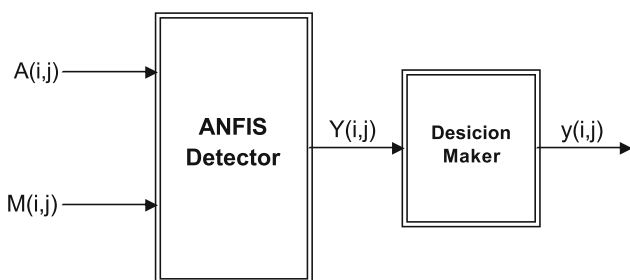


Fig. 2. The general structure of the proposed neuro-fuzzy IN detection operator.

process. First, the consequent parameters are identified using LSM when the values of premise parameters are fixed. After that, the consequent parameters are held fixed while the error is propagated from the output end to the input end, and the premise parameters are updated by the Standard BP algorithm.

3. Proposed impulse detector

Block diagram of the proposed ANFIS detector is shown in Fig. 2. In this figure, input variables of the ANFIS are luminance value of the pixel $A(i,j)$ at position (i,j) and median of the luminance values of the neighbor pixels in the 3×3 analysis window $M(i,j)$. $Y(i,j)$ represents the output value of the detector.

ANFIS detector is a first order Sugeno type fuzzy system with two inputs and one output. Six *triangular* type membership functions are used for all input variables whereas a linear membership function is used for output variable. The output of the ANFIS is applied to decision maker. The output of the decision maker is calculated as follows:

$$y(i,j) = \begin{cases} L_{\min} & \text{if } Y(i, j) < \frac{L_{\min} + L_{\max}}{2} \\ L_{\max} & \text{if } Y(i, j) \geq \frac{L_{\min} + L_{\max}}{2} \end{cases} \quad (10)$$

where L_{\min} and L_{\max} represent the minimum and the maximum values of the allowable dynamic luminance range, respectively. For 8-bit images, L_{\min} is 0 and L_{\max} is 255.

The ANFIS detector requires a training data set and testing data set. Training data sets are used to specify the detector structure

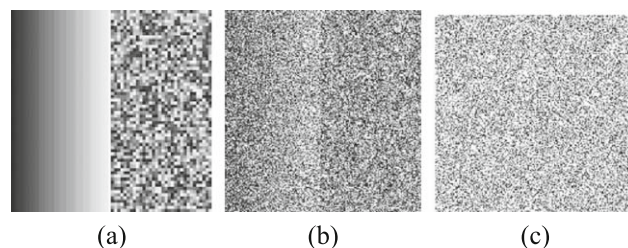


Fig. 3. Training images: (a) base training image; (b) input training image; (c) target training image.

and parameters, whereas the testing data sets are used in final testing of the detector. Fig. 3(a) shows the original training image, which is a 256×256 pixel artificial training image can easily be generated in a computer [26]. Each square box in this image has a size of 4×4 pixels and the 16 pixels contained within each box have the same luminance value, which is a random integer number uniformly distributed in $[0, 255]$. The input training image shown in Fig. 3(b) is obtained by simply corrupting the base training image by IN of 70% noise density. The target training image shown in Fig. 3(c) is a difference image obtained from the base training image and the input training image. Luminance values of its pixels are obtained by subtracting the luminance values of the pixels of the input training image from luminance values of the corresponding pixels of the base training image, and then converting the nonzero values to white pixels and zero values to black pixels. Hence, the locations of the white pixels in the target training image correspond to the locations of the corrupted pixels in the input training image.

The parameters of the ANFIS are then iteratively tuned by using the hybrid learning algorithm [29,30] so as to minimize the learning error. The epoch number, which is the number of times the complete training set has been trained, was selected as 10 for training. The hybrid learning algorithm can dramatically reduce the required training epochs because the training errors are decoupled and treated separately. It was observed that when the epoch number increases, performance of the ANFIS detector does not change significantly. The number of membership functions for the both input variables are 6. The number of rules is then 36 ($6 \times 6 = 36$). The triangular MF is specified by three parameters seen from Eq. (4). Therefore, the ANFIS used here contains a total of 144 fitting parameters, of which $36 (6 \times 6 + 6 \times 3 = 36)$ are the

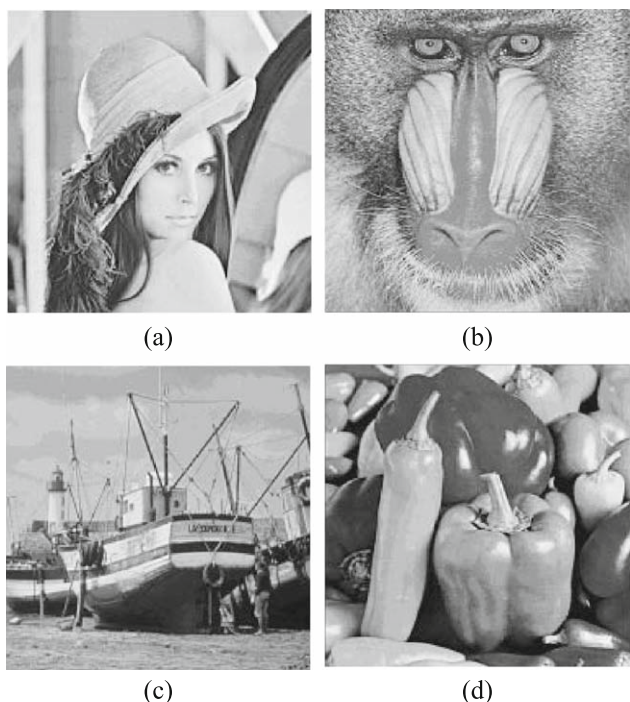


Fig. 4. Test images: (a) Lena; (b) Baboon; (c) Boats; (d) Peppers.

premise parameters and 108 ($3 \times 36=108$) the consequent parameters. Once the training of the ANFIS is completed, its internal parameters are fixed. After proper training, ANFIS completely bypasses the repeated use of complex iterative processes for new cases presented to it. Even if training takes a few minutes, the test process takes only a few microseconds to detect IN of different test images.

After the detection step is completed, filtering step is realized similar to [14]. Corrupted pixels detected with the proposed detector are discarded from 3×3 sliding window W . Then, the median luminance value of the remaining pixels within W is computed and luminance value of the corrupted pixel is changed with computed median value. If all pixels within the W are corrupted with IN, then the window size of W is increased until at least one pixel remained within the sliding window.

The main steps of the proposed method can be summarized as follows:

1. Form training inputs $A(i,j)$ and $M(i,j)$ using artificial training image by IN of 70% noise density. Subtract the luminance values of the pixels of the input training image from luminance values of the corresponding pixels of the base training image, and then convert the nonzero values to white pixels and zero values to black pixels to obtain target training image. (The locations of the white pixels correspond to the corrupted pixels.)

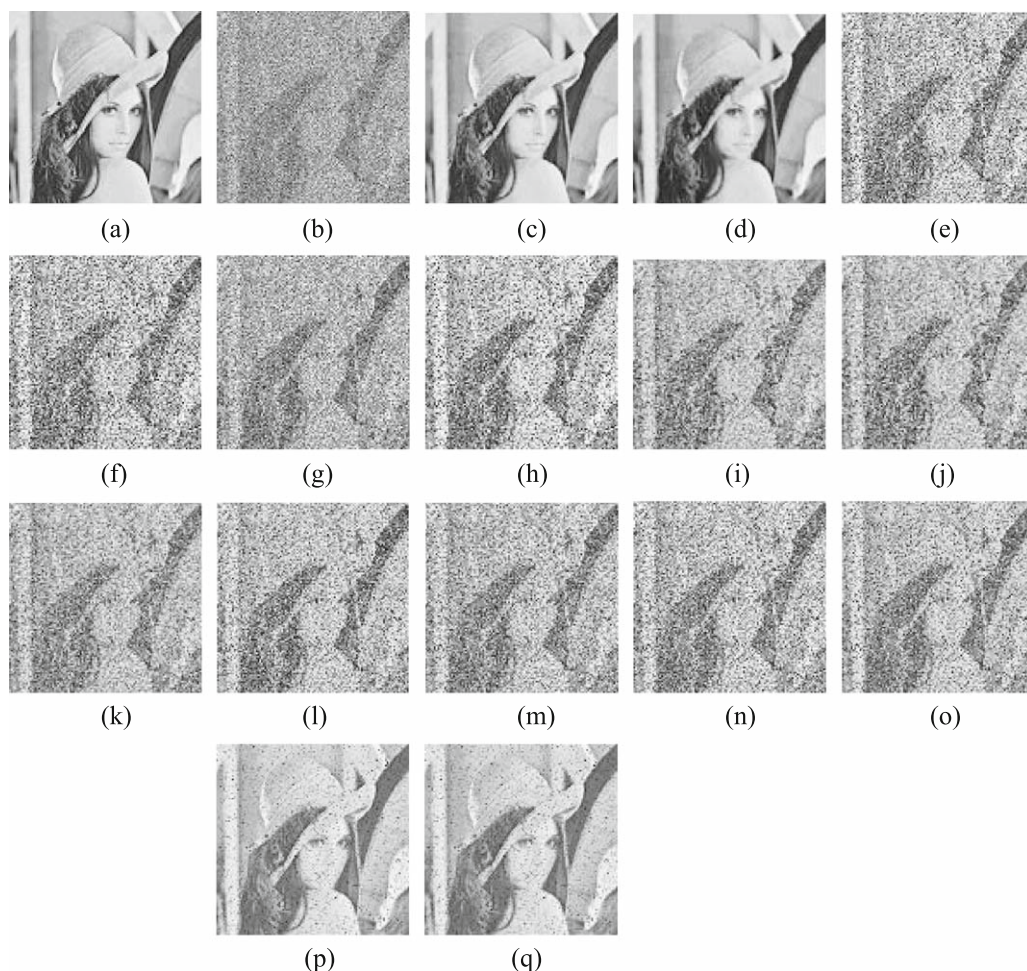


Fig. 5. Output images of the operators for the *Lena* image corrupted by impulse noise with 70% noise density: (a) Original *Lena* image; (b) Noisy *Lena* image; (c) NFDMF (proposed); (d) NNDMF; (e) CWM; (f) TSM; (g) LUM; (h) FSB; (i) IFCF; (j) MIFCF; (k) EIFCF; (l) SFCE; (m) FIRE; (n) PWLFIRE; (o) FMF; (p) AWFM; (q) ATMAV.

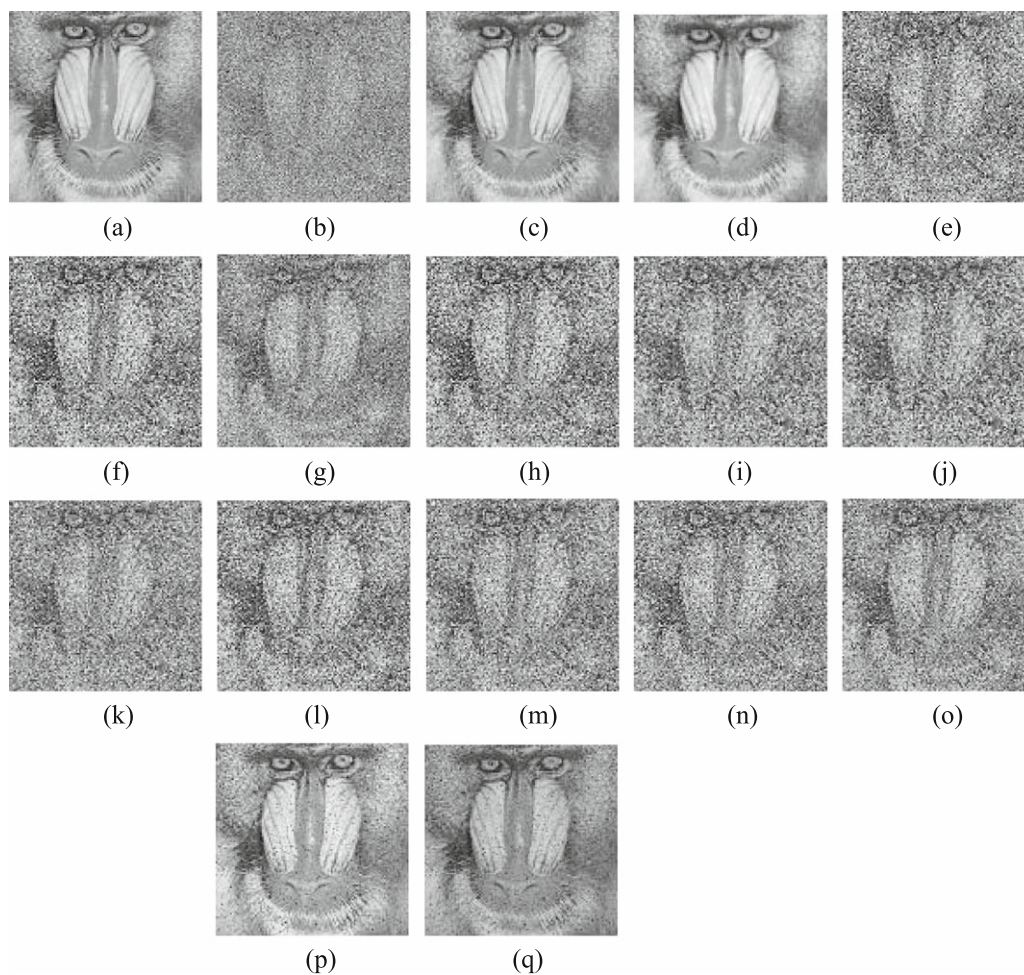


Fig. 6. Output images of the operators for the *Baboon* image corrupted by impulse noise with 70% noise density: (a) original *Baboon* image; (b) noisy *Baboon* image; (c) NFDMF (proposed); (d) NNDMF; (e) CWM; (f) TSM; (g) LUM; (h) FSB; (i) IFCF; (j) MIFCF; (k) EIFCF; (l) SFCF; (m) FIRE; (n) PWLFIRE; (o) FMF; (p) AWFM; (q) ATMAV.

Table 1

PSNR values of the proposed filter and comparison filters for the *Lena* test image at different noise density.

Method	Noise density							
	%10	%20	%30	%40	%50	%60	%70	%80
Noisy	14.8	11.8	10.0	8.6	7.8	7.0	6.4	5.8
NFDMF	43.2	39.8	37.6	35.8	34.0	32.3	30.3	27.6
NNDMF	32.3	32.0	31.5	30.0	28.9	27.7	26.1	23.6
CWM	33.4	25.4	19.6	15.4	12.4	10.2	8.4	7.0
TSM	22.9	25.5	19.5	15.3	12.2	9.9	8.0	6.5
LUM	26.3	18.8	14.5	11.7	9.7	8.1	7.0	6.1
FSB	33.7	28.9	23.0	18.1	14.3	11.5	9.3	7.4
IFCF	32.6	29.0	25.0	21.3	18.1	15.6	13.5	11.7
MIFCF	32.2	29.1	25.2	21.4	18.2	15.6	13.3	11.5
EIFCF	31.0	30.0	23.1	19.5	16.7	14.4	12.6	11.0
SFCF	29.5	24.4	27.6	16.8	14.1	12.0	10.2	8.7
FIRE	29.9	23.2	18.8	15.5	12.8	10.9	9.3	7.9
PWLFIRE	28.0	21.3	17.1	13.8	11.4	9.6	8.0	6.7
FMF	36.2	29.9	23.7	18.6	15.1	12.4	10.3	8.6
AWFM	26.2	26.0	25.7	25.3	24.1	21.8	16.3	11.3
ATMAV	28.7	29.9	30.2	29.6	26.8	21.6	16.2	11.2

2. Train the ANFIS structure for 10 epochs using data set formed in step 1.
3. Form test inputs $A(i,j)$ and $M(i,j)$ for any noisy test images.
4. Compute ANFIS output for test inputs using ANFIS trained in step 2.
5. Apply ANFIS output to decision maker as shown in Fig. 2. Determine the decision maker output using Eq. (10). If the output of the decision maker is 255 for pixel at position (i,j) , then this pixel corrupted with IN.
6. Realize filtering step described above for all corrupted pixels.

Table 2
PSNR values of the proposed filter and comparison filters for the *Baboon* test image at different noise density.

Method	Noise density							
	%10	%20	%30	%40	%50	%60	%70	%80
Noisy	15.5	12.5	10.8	9.6	8.6	7.8	7.1	6.5
NFDMF	32.3	29.3	27.4	26.0	24.7	23.6	22.5	21.3
NNDMF	22.7	22.6	22.5	22.3	22.0	21.6	21.2	20.5
CWM	25.3	22.4	18.8	15.4	12.8	10.8	9.0	7.6
TSM	24.9	22.4	18.7	15.2	12.5	10.3	8.5	7.2
LUM	23.7	18.4	14.7	12.1	10.1	8.7	8.7	6.7
FSB	23.0	22.1	20.0	17.1	14.3	11.9	9.8	8.0
IFCF	23.5	22.0	20.1	18.0	15.8	14.1	12.7	11.8
MIFCF	23.2	21.9	20.1	17.8	15.6	13.8	12.3	11.4
EIFCF	22.7	20.7	18.7	16.5	14.7	13.2	11.9	11.2
SFCF	26.3	22.8	19.5	16.5	14.1	12.2	10.6	9.4
FIRE	24.9	21.4	18.1	15.3	13.1	11.3	9.8	8.6
PWLFIRE	26.8	21.1	17.2	14.2	12.0	10.2	8.7	7.4
FMF	26.9	23.6	20.6	17.5	14.8	12.6	10.8	9.3
AWFM	22.4	22.3	22.2	21.9	21.3	19.9	17.0	13.3
ATMAV	22.6	22.3	22.3	22.2	21.8	20.2	17.2	13.3

Table 3
MAE values of the proposed filter and comparison filters for the *Boats* test image at different noise density.

Method	Noise density							
	%10	%20	%30	%40	%50	%60	%70	%80
Noisy	12.7	25.5	38.2	50.9	64	76.7	89.1	105.2
NFDMF	0.6	1.2	1.8	2.5	3.4	4.5	6.0	8.5
NNDMF	6.0	6.2	6.5	7.0	7.6	8.7	10.1	12.8
CWM	2.5	4.0	7.7	14.7	25.3	40.1	57.9	80.1
TSM	1.2	2.7	6.7	14.2	26.1	42.8	63.3	88.0
LUM	2.3	7.0	15.8	27.7	42.7	58.9	75.7	93.6
FSB	4.5	5.3	7.1	11.4	19.6	32.7	51.0	73.5
IFCF	5.0	6.7	10.1	15.6	23.5	33.0	43.1	52.5
MIFCF	5.2	6.8	9.9	15.3	23.2	33.2	44.0	53.9
EIFCF	5.3	7.8	12.1	18.7	27.5	37.4	47.8	56.9
SFCF	6.1	9.0	14.2	22.3	32.9	44.6	56.6	67.5
FIRE	1.7	4.7	10.0	18.3	29.6	43.7	59.9	76.4
PWLFIRE	0.8	3.1	7.8	15.7	27.1	41.8	59.9	80.3
FMF	1.5	3.2	6.2	11.9	21.1	34.0	49.9	67.1
AWFM	5.3	5.5	5.6	5.8	6.3	7.8	12.2	25.1
ATMAV	5.7	6.0	6.0	6.1	6.4	7.8	12.3	25.3

Table 4
MAE values of the proposed filter and comparison filters for the *Peppers* test image at different noise density.

Method	Noise density							
	%10	%20	%30	%40	%50	%60	%70	%80
Noisy	12.7	25.7	38.2	50.9	63.6	76.9	89.5	102.5
NFDMF	0.6	0.9	1.4	2.3	3.0	4.0	5.2	7.2
NNDMF	4.2	4.4	4.6	4.9	5.4	6.2	7.5	9.9
CWM	1.9	3.3	6.8	13.6	24.3	38.7	57.8	78.9
TSM	0.6	2.1	5.8	13.0	24.8	41.2	63.0	86.6
LUM	2.0	6.5	15.2	27.2	42.1	58.2	75.8	93.2
FSB	3.4	4.1	5.7	9.9	18.2	31.4	49.9	72.8
IFCF	3.6	5.2	8.4	14.1	22.3	32.4	43.4	53.4
MIFCF	3.8	5.3	8.2	13.7	22.0	32.6	44.6	55.2
EIFCF	3.9	6.2	10.4	17.2	25.6	37.3	48.4	58.1
SFCF	5.2	8.2	13.6	22.1	32.9	44.9	56.9	67.8
FIRE	1.3	4.2	9.2	17.4	28.9	43.1	59.3	75.9
PWLFIRE	0.8	3.0	7.5	15.3	26.8	41.6	59.6	80.1
FMF	0.9	2.2	4.6	10.1	19.4	32.7	48.8	66.3
AWFM	33.1	51.8	64.3	72.3	77.2	80.7	83.3	86.6
ATMAV	4.2	4.5	4.5	4.5	4.7	5.7	9.1	18.8

Table 5
Runtimes of the mentioned methods for the *Baboon* image for different IN levels.

Method	Runtime (s)	
	% 10	% 80
CWM	9.2	8.7
TSM	18.1	18.0
LUM	3.6	3.2
FSB	165.9	166.4
IFCF	783.0	850.2
MIFCF	833.7	809.8
EIFCF	919.6	906.2
SFCF	323.6	317.9
FIRE	277.2	274.1
PWLFIRE	22.8	22.3
FMF	2.0	2.12
AWFM	143.9	144.6
ATMAV	24.9	24.6
NNDMF	2.56	2.58
NFDMF	0.6	3.1

4. Simulation results

The performance of the proposed method is tested under various noise conditions and on several popular images from the literature including *Lena*, *Baboon*, *Boats*, and *Peppers*. These images, which are 8-bit gray level images having the same size of 512×512 pixels, are shown in Fig. 4. The test images used in the experiments are generated by contaminating the original images by IN with an appropriate noise ratios ranging from 10% to 80% with an increment step of 10%.

For comparison, the corrupted test images are also filtered by using several conventional and state-of-the-art IN removal operators including CWM [4], TSM [5], LUM [6], FSB [15] (fuzzy similarity filter), IFCF [16], MIFCF [16], EIFCF [16], SFCF [17], FIRE [18], PWLFIRE [19], FMF [20,21] (fuzzy median filter), AWFM [22,23], and ATMAV [24]. In order to show performance of the ANFIS with respect to the neural network [31], the NFDMF results are also compared with the neural network detector median filter (NNDMF) results. The multilayer perceptron (MLP) network architecture was used in NNDMF. In MLP, the most suitable network configuration was two hidden layer with three neurons. In order to train MLP, the Levenberg–Marquardt learning algorithm [32] was used.

Restoration performances are quantitatively measured by the peak signal-to-noise ratio (PSNR) which is defined as

$$PSNR = 10 \log_{10} \left(\frac{255^2}{MSE} \right) \text{dB} \quad (11)$$

where mean-squared-error (MSE) is defined as

$$MSE = \frac{1}{MN} \sum_{i=1}^M \sum_{j=1}^N [org(i,j) - img(i,j)]^2 \quad (12)$$

where *org* is the original image, *img* is the filtered image of size *MN*. In addition, the mean absolute error (MAE) has also been taken as a quantitative measure to evaluate the levels of the edges and the details preserved, which is defined as

$$MAE = \frac{1}{MN} \sum_{i=1}^M \sum_{j=1}^N |org(i,j) - img(i,j)| \quad (13)$$

The restoration results for the *Lena* and *Baboon* test images corrupted with 70% IN are illustrated in Figs. 5 and 6, respectively. It is clearly seen from these figures that the proposed filter preserves edge sharpness and reduces many artifacts, even if the noise density is high. The PSNR values of the filters have also been

given in Tables 1 and 2 for making quantitative evaluation for *Lena* and *Baboon* test images. It is clearly seen from Tables 1 and 2 that the proposed NFDMF generates the best PSNR values. The MAE values for *Boats* and *Peppers* test images have been given in Tables 3 and 4. It is clear from Tables 3 and 4 that the proposed NFDMF shows better performance than other filters in the sense of being effective in noise suppression and detail preservation, especially when the noise density is very high.

Another important requirement of the modern image enhancement filters is robustness. Tables 1–4 indicate that the proposed NFDMF provides robustness substantially across a wide variation of noise ratios.

In order to evaluate the computational complexities, the runtimes of all the mentioned filters for *Baboon* image for different IN levels were determined and given in Table 5. The runtime analysis of the proposed NFDMF and concerned filters were conducted for test images using a Pentium IV, 3 GHz PC. It is seen from Table 5 that NFDMF is one of the fastest algorithms.

5. Conclusion

In this paper, an IN detector based on ANFIS is proposed. It can be seen from Figs. 5 and 6 that proposed NFDMF gives absolutely better restoration results in the restored images when compared with the IN suppression filters mentioned in this paper.

The advantages of the proposed filter may be summarized as follows.

1. The implementation of the method is very easy. It is based on a simple 2-input 1-output NF system.
2. The internal parameters of the NF system are determined by training. Training of the system can easily be realized by using artificial images generated in computer.
3. The NFDMF supplies superior restoration results compared to both median based filters (CWM, TSM, and LUM) and recently introduced fuzzy based filters (FSB, IFCF, MIFCF, EIFCF, SFCF, FIRE, PWLFIRE, FMF, AWFM, and ATMAV). The NFDMF is also better than the NNFMF.
4. The runtime of the proposed filter is less than most of the comparison filters. Finally, proposed method is easy to implement and has a very low execution time.

Acknowledgment

Author is grateful to Dr. Stefan Schulte for sending her source codes of the comparison filters mentioned in the paper.

References

- [1] Bovik A. Handbook of image and video processing. New York: Academic; 2000.
- [2] Huang TS, Yang GJ, Tang GY. Fast two-dimensional median filtering algorithm. IEEE Trans Acoust Speech Signal Process 1979;1(1):13–8.
- [3] Nodas TA, Gallagher NCJ. The output distribution of median type filters. IEEE Trans Commun 1984;32(5):532–41.
- [4] Ko SJ, Lee YH. Center weighted median filters and their applications to image enhancement. IEEE Trans Circuits Syst 1991;38(9):984–93.
- [5] Chen T, Ma KK, Chen LH. Tri-state median filter for image denoising. IEEE Trans Image Process 1999;8(12):1834–8.
- [6] Hardie RC, Boncelet CG. Lum filters: a class of rank-order-based filters for smoothing and sharpening. IEEE Trans Signal Process 1993;41(3):1834–8.
- [7] Lukac R. Binary lum smoothing. IEEE Signal Process Lett 2002;19:400–3.
- [8] Lukac R, Plataniotis KN, Smolka B, Venetsanopoulos AN. Generalized selection weighted vector filters. EURASIP J Appl Signal Process 2004;2004(12): 1870–85.
- [9] Eng H, Ma KK. Noise adaptive soft-switching median filter. IEEE Trans Image Process 2001;10(2):242–51.

- [10] Paul ME, Bruce K. C language algorithms for digital signal processing. Upper Saddle River, NJ: Prentice-Hall; 1991.
- [11] Sun T, Neuvo Y. Detail-preserving median based filters in image processing. *Patten Recognition Lett* 1994;15(4):341-7.
- [12] Lin H, Willson AN. Median filter with adaptive length. *IEEE Trans Circuits Syst* 1988;35(6):675-90.
- [13] Wang Z, Zhang D. Progressive switching median filter for the removal of impulse noise from highly corrupted images. *IEEE Trans Circuits Syst* 1999;46(1):78-80.
- [14] Besdok E, Yuksel ME. Impulsive noise suppression from images with Jarque Bera test based median filter. *Int J Electron Commun (AE)* 2005;59:105-10.
- [15] Kalaykov I, Tolt G. Real-time image noise cancellation based on fuzzy similarity. *Fuzzy filters for image processing*, 1st ed.. Heidelberg, Germany: Physica Verlag; 2003. p. 54-71.
- [16] Farbiz F, Menhaj MB. A fuzzy logic control based approach for image filtering. In: Kerre E, Nachttegael M, editors. *Fuzzy techniques in image processing*, 1st ed. Heidelberg, Germany: Physica Verlag; 2000. p. 194-221.
- [17] Farbiz F, Menhaj MB, Motamedi SA. Edge preserving image filtering based on fuzzy logic. In: 6th EUFIT conference, 1998. p. 1417-21.
- [18] Russo F, Ramponi G. A fuzzy filter for images corrupted by impulse noise. *IEEE Signal Process Lett* 1996;3(6):168-70.
- [19] Russo F. Fire operators for image processing. *Fuzzy Sets Syst* 1999;103(2):265-75.
- [20] Arakawa K. Median filter based on fuzzy rules and its application to image restoration. *Fuzzy Sets Syst* 1999;103:265-75.
- [21] Arakawa K. Fuzzy rule-based image processing with optimization. In: Kerre EE, Nachttegael M, editors. *Fuzzy techniques in image processing*, 1st ed. Heidelberg, Germany: Physica Verlag; 2000. p. 222-47.
- [22] Lee CS, Kuo YH, Yu PT. Weighted fuzzy mean filters for image processing. *Fuzzy Sets Syst* 1997;89:157-80.
- [23] Lee CS, Kuo YH. Adaptive fuzzy filter and its application to image enhancement. In: Kerre EE, Nachttegael M, editors. *Fuzzy techniques in image processing*, 1st ed. Heidelberg, Germany: Physica Verlag; 2000. p. 172-93.
- [24] Kwan HK. Fuzzy filters for noise reduction in images. In: Nachttegael M, Van der Weken D, Van De Ville D, Kerre EE, editors. *Fuzzy filters for image processing*, 1st ed.. Heidelberg, Germany: Physica Verlag; 2003. p. 25-53.
- [25] Yuksel ME, Basturk A. Efficient removal of impulse noise from highly corrupted digital images by a simple neuro-fuzzy operator. *Int J Electron Commun (AE)* 2003;57(3):214-9.
- [26] Yuksel ME. A median/anfis filter for efficient restoration of digital images corrupted by impulse noise. *Int J Electron Commun (AE)* 2006;60:628-37.
- [27] Toprak A, Ozerdem MS, Guler I. Suppression of impulse noise in mr images using artificial intelligent based neuro-fuzzy adaptive median filter. *Digital Signal Process* 2008;18(3):391-405.
- [28] Yildirim MT, Basturk A, Yuksel ME. Impulse noise removal from digital images by a detail-preserving filter based on type-2 fuzzy logic. *IEEE Trans Fuzzy Syst* 2008;16(4):920-8.
- [29] Jang JSR. *Anfis: Adaptive-network-based fuzzy inference system*. *IEEE Trans Systems Man Cybernetics* 1993;23:665-85.
- [30] Jang JSR, Sun CT, Mizutani E. *Neuro-fuzzy and soft computing: a computational approach to learning and machine intelligence*. Upper Saddle River, NJ: Prentice-Hall; 1997.
- [31] Haykin S. *Neural networks: a comprehensive foundation*. New York: Macmillan College Publishing Company; 1994.
- [32] Hagan MT, Menhaj M. Training feedforward networks with the Marquardt algorithm. *IEEE Trans Neural Networks* 1994;5(6):989-93.



Ilke Turkmen was born in Kayseri, Turkey, on December 26, 1976. She received B.S., M.S., and Ph.D. degrees in electronics engineering from Erciyes University, Kayseri, Turkey, in 1997, 1999, and 2005, respectively. Currently, she is an assistant professor at the Department of Aircraft Electrical and Electronics of Civil Aviation School, Erciyes University. Her current research activities include neural networks, intelligent algorithms, fuzzy inference systems, and their applications to target tracking and image processing.